Research Square

Preprints are preliminary reports that have not undergone peer review.
They should not be considered conclusive, used to inform clinical practice,
or referenced by the media as validated information.

Toe Orientation Alters Load Distribution and Coordination Patterns during Badminton Lunge Landing

Jun Wen
Ningbo University
Zilong Lu
Ningbo University
Zirui Yin
Ningbo University
Pengbin Tong
Ningbo University
Enze Shao
Ningbo University
Bálint Kovács
Hungarian University of Sports Science
Dong Sun
Ningbo University
Yang Song
Ningbo University
Tibor J. Goda
Obuda University
Fei Zheng
Anta (China) Co
Junxia Lin
Anta (China) Co
Peng Yang
nbupengyang@outlook.com

Ningbo University

Research Article

Keywords: Badminton lunge, Foot rotation position, Lower extremity biomechanics, Kinetic chain coordination, Cross-correlation analysis, Finite element modeling

Posted Date: July 25th, 2026

DOI: https://doi.org/10.21203/rs.3.rs-10392752/v1

License: This work is licensed under a Creative Commons Attribution 4.0 International License.
Read Full License

Additional Declarations: No competing interests reported.

Abstract

Background

Toe orientation during badminton lunge landing may influence lower-extremity biomechanical coordination and knee joint loading, potentially affecting injury risk. This study aimed to examine inter-joint coordination and tissue-level stress responses under different toe orientations during badminton lunge landing using cross-correlation analysis and subject-specific finite element analysis (FEA).

Methods

Thirty male recreational badminton players (21.70 ± 1.20 years, 175.67 ± 2.53 cm, 65.72 ± 4.08 kg) performed right-leg lunge landings with 20° toe-in orientation (TIO) and toe-out orientation (TOO) in randomized order. Kinematic and kinetic data were collected using three-dimensional motion capture and force platforms. Knee models from eight participants were reconstructed from CT and MRI, and joint forces were applied for FEA.

Results

Compared with TOO, TIO showed greater ankle dorsiflexion and eversion ($p < 0.001$) and higher ankle and knee joint reaction forces in the late phase (94–100%, $p = 0.045$), with increased sagittal-plane center of mass displacement ($p = 0.023$). TOO demonstrated greater knee abduction angles ($p = 0.048$–0.007) and higher initial ground reaction force (0–5%, $p = 0.048$). Coordination differences were observed in ankle motion–knee loading interactions ($p = 0.038$–0.003). FEA revealed higher peak stress and more concentrated stress distribution in knee tissues under TIO, particularly in the medial compartment.

Conclusions

Toe orientation markedly modulates kinetic chain coordination and knee stress during badminton lunge landing. TIO increases load concentration across multiple knee structures, whereas TOO facilitates load redistribution and reduces internal tissue stress, suggesting a potential strategy for injury risk reduction.

1 Introduction

Badminton is characterized by frequent high-intensity and multidirectional movements that impose substantial mechanical loads on the lower extremities, contributing to a high incidence of non-contact injuries [1, 2]. Among these movements, the forward lunge is one of the most commonly performed and mechanically demanding tasks, generating impact loads of approximately 2.5 times body weight during landing [3, 4]. As primary load-bearing structures within the lower-limb kinetic chain, the ankle and knee joints are therefore particularly vulnerable to injury during lunge landings.

Foot orientation at initial contact has been identified as a key factor influencing lower-limb biomechanics. Previous studies have shown that toe rotation can substantially alter joint kinematics and loading patterns. For instance, toe-out landing has been reported to reduce strain on the anterior talofibular ligament in individuals with chronic ankle instability [5], whereas studies on single-leg landing tasks have suggested that externally rotated foot positions may increase knee valgus angles and moments, potentially elevating loading on structures such as the anterior cruciate ligament (ACL) [6]. Similarly, evidence from cutting maneuvers indicates that foot positioning is associated with knee injury risk [7]. These seemingly conflicting findings suggest that the biomechanical effects of toe orientation may be task-specific and cannot be fully explained by isolated joint-level analyses.

One potential explanation lies in the coordinated behavior of the lower-limb kinetic chain. Joint coupling analysis has been widely used to characterize inter-joint coordination by quantifying spatiotemporal relationships between joint motions [8, 9]. Previous studies have demonstrated that distal joint motions can influence proximal joint mechanics through coupling mechanisms [10], and that ankle kinematics are associated with changes in knee motion in the frontal and transverse planes [11]. In addition, distinct coordination patterns across the ankle, knee, and hip have been identified, with certain patterns linked to increased knee valgus loading [12]. However, most existing studies have focused on kinematic-level coordination, with limited attention to how such temporal coordination influences the internal mechanical environment of the knee joint.

From a whole-body perspective, maintaining dynamic stability during landing requires coordinated regulation of the center of mass (COM). The motion of the COM has been shown to reflect global balance control and is closely associated with lower-limb joint function [13, 14]. During badminton lunge landings, alterations in foot orientation have been associated with changes in ankle kinematics and COM displacement [15], suggesting that local joint adjustments may serve to regulate overall stability. This implies that ankle–knee coordination and COM dynamics may be functionally linked as part of a compensatory control strategy. However, whether such coordination patterns lead to meaningful changes in internal knee joint loading remains unclear.

Cross-correlation analysis provides a useful approach for quantifying the temporal relationships between biomechanical variables by identifying the strength and time lag of their interactions [16]. This method has been applied to examine neuromechanical delays and inter-joint coordination in gait and clinical populations. Nevertheless, cross-correlation analysis is limited to describing temporal associations and does not provide insight into tissue-level mechanical responses. To address this limitation, finite element analysis (FEA) enables the estimation of internal stress and strain distributions within joint structures under specific loading conditions and has been widely applied to investigate joint mechanics during dynamic tasks such as landing [17]. Integrating these approaches may therefore provide a means to link inter-joint coordination with intra-articular biomechanics.

Therefore, the present study aims to investigate the biomechanical interactions of the lower-limb kinetic chain during badminton lunge landings by combining cross-correlation analysis and finite element

modeling. Specifically, this study seeks to (1) quantify the temporal coupling between ankle–knee joint motion and COM dynamics under different toe orientations, and (2) evaluate the corresponding changes in internal knee joint stress distributions using subject-specific finite element models. By establishing a cross-scale linkage between inter-joint coordination and intra-articular mechanical responses, this study extends beyond previous work that focused solely on kinematic or kinetic outcomes. It is hypothesized that moderate toe-out landing may reduce knee joint loading while maintaining dynamic stability, and that significant temporal coupling exists between joint motion and COM behavior.

2 Methods

2.1 Participants

The required sample size was calculated using G*Power software (version 3.1.9.7; Heinrich Heine University Düsseldorf, Germany). Based on a one-way repeated measures ANOVA (effect size f = 0.25, α = 0.05, power = 0.85), a minimum of 28 participants was required to ensure sufficient statistical power. Thirty male recreational badminton players (21.70 ± 1.20 years, 175.67 ± 2.53 cm, 65.72 ± 4.08 kg) from a local university were recruited to participate in this study.

To ensure sample homogeneity, the following inclusion criteria were applied: (1) healthy male university students; (2) engagement in badminton 3–4 times per week, with each session lasting at least 2 hours; (3) no history of lower limb injuries within the preceding 6 months and no illnesses affecting athletic performance; (4) dominant right leg and right hand. All participants were fully informed of the study objectives, procedures, requirements, and provided written informed consent prior to participation. The study protocol was approved by the institutional ethics committee (Approval No.: TY 2025051).

2.2 Experimental protocol and procedure

2.2.1 Experimental setup

This experiment was conducted at the Biomechanics Laboratory of the University. Prior to testing, participants' height and weight were measured as baseline anthropometric data, and right leg length (from the lateral malleolus to the anterior superior iliac spine) was also measured [18]. Stride length for each participant was calculated based on their right leg length, serving as the standard for performing a complete and proper lunge landing. For kinematic measurements 38 reflective markers (12.5 mm in diameter) were placed on the participants' key bony landmarks following the OpenSim Gait2392 musculoskeletal model. 3D kinematic data were collected using a 10-camera Vicon (Oxford Metrics Ltd., Oxford, UK) sampling at 200 Hz. In addition, the tests were performed on an embedded force plate (Kisler Instruments AG, Winterthur, Switzerland) to measure vertical ground reaction forces synchronously with the motion capture at 1000 Hz [19]. During testing, participants wore close-fitting sportswear to prevent clothing from obscuring marker points. All participants wore a new pair of Yonex badminton shoes (Yonex Power Cushion 65 Z, model code: SHB-65Z3) to standardize footwear conditions.

2.2.2 Experimental procedure

Prior to formal data collection, participants completed a standardized 15-minute warm-up under the supervision of a professional strength and conditioning coach. The warm-up protocol consisted of dynamic stretching, sport-specific task i.e., and warm-up running. Afterward standard gymnastic warm up tasks were performed. After warm-up, participants performed several familiarization trials to practice the standardized right-lunge movement.

During the experiment, participants executed a standardized right lunge by stepping forward from point A to landing point B, followed by pushing back to point A after right-leg landing (Fig. 1C). To simulate real match conditions and control technical variables, two landing toe-direction conditions were established: internal rotation (20° toe-in orientation, TIO) and external rotation (20° toe-out orientation, TOO) (Fig. 1B) [15]. The target angles were marked on the force plate using adhesive tape to ensure accurate foot placement. Prior to each trial, the landing orientation (inward or outward) was randomly assigned using a custom MATLAB (R2025b, The MathWorks Inc., Natick, MA, USA) program to minimize potential learning effects during task execution. Each participant completed seven valid lunge trials under each toe-direction condition, with a two-minute rest interval between trials to minimize fatigue effects. Trials in which the participant's right foot did not fully contact the force plate were considered invalid and excluded from further analysis.

2.3 Data processing and analysis

A blinded analysis procedure was employed to mitigate potential confirmation bias during data processing, in which analysts may place greater emphasis on results aligning with expected outcomes when group assignments are known. Data processing was performed without knowledge of the toe-direction groupings to minimize subjective influence on parameter extraction and interpretation.

Initial contact was defined as the instant when vertical ground reaction force (GRF) first exceeded 10 N, and toe-off as the instant when it subsequently fell below 10 N. The interval between initial contact and toe-off was defined as the landing phase, and all kinetic analyses were performed over this phase. For each participant, data from seven successful trials were averaged for subsequent analysis. Kinematic and kinetic data were exported from Vicon Nexus 2.19 (Vicon, Oxford Metrics Inc., Oxford, UK) in C3D format and converted into TRC and MOT files using a custom MATLAB script (R2025a, The MathWorks, MA, USA). Signal processing followed the procedures recommended by Winter [20, 21]. Specifically, GRF data were filtered using a fourth-order zero-lag Butterworth low-pass filter with a cutoff frequency of 20 Hz, while kinematic data were filtered using a cutoff frequency of 10 Hz. The processed data were then imported into OpenSim 4.5.2 (SimTK, Stanford, USA) for musculoskeletal modelling and biomechanical analysis. A generic musculoskeletal model (Gait2392) was scaled according to each participant’s anthropometric data, and muscle attachment locations were adjusted to ensure anatomical consistency. Joint kinematics were calculated using inverse kinematics. To improve the dynamic consistency between the model and experimental data, the tool of residual reduction algorithm was applied to minimize residual forces, acting on the COM in the frontal and transverse planes. Subsequently, joint

moments for each degree of freedom were calculated using inverse dynamics. Joint power was then obtained by multiplying joint moments by the corresponding angular velocities. Finally, ankle and knee joint reaction forces ($F_{reaction}$) were calculated using the OpenSim 4.5.2 (SimTK, Stanford, USA) [22]. GRF, joint kinematics, and segment inertial parameters were applied to the musculoskeletal model to estimate the net reaction forces acting at the ankle and knee joints.

To eliminate the influence of individual body mass differences, all joint reaction forces were normalized to body weight, and time was normalized to 0–100% of the contact phase.

2.4 Cross-correlation analysis

Cross-correlation coefficients were calculated between joint biomechanical parameter curves to assess ankle–knee joint coupling. A custom MATLAB (R2025a) script was employed to compute the cross-correlation functions between biomechanical variables. Within the defined lag range, the cross-correlation coefficient with the maximum absolute value and its corresponding lag were extracted. Cross-correlation coefficients range between − 1 and 1, where positive values indicate similar trends in variable changes and negative values indicate opposite trends. A larger absolute value indicates stronger coupling between variables [16].

Given that the lower limb kinetic chain plays a dominant role during landing in the lunge position, this study selected time-series biomechanical variables, including COM displacement (COMx: anterior–posterior displacement of the center of mass; COMy: medial–lateral displacement of the center of mass), ankle dorsiflexion angle (ADF), ankle eversion angle (AEV), knee extension angle (KEX), knee abduction angle (KAB), ankle and knee joint reaction forces (ARF: ankle reaction force; KRF: knee reaction force), ankle and knee joint sagittal-plane shear forces (ASF: ankle sagittal shear force; KSF: knee sagittal shear force), and vertical ground reaction force (GRF) for cross-correlation analysis [12].

2.5 FEA of the knee joint

2.5.1 Geometry acquisition and reconstruction

This study selected eight participants with no history of injury or pathology in the right knee joint within the preceding six months. Three-dimensional geometric models of the participants' right knee joints were constructed from CT (scan reconstruction layer thickness: 0.5 mm; 120 kV, 250–300 mA) and MRI (GE Discovery-sim 750, with the built-in body coil) imaging data to reconstruct the anatomical structures of bones, cartilage, and ligaments. The CT scan parameters were as follows: tube voltage 120 kV, current 125 mA, slice thickness 2 mm, and no interslice gap. MRI data were used to identify soft tissue structures and the anatomical attachment sites of ligaments. Initially, Mimics 21.0 (Materialise, Leuven, Belgium) was employed to segment the two-dimensional imaging sequences to extract bony structures, including the femur, tibia, and patella, and reconstruct their high-fidelity three-dimensional geometric surfaces. Cartilage was reconstructed based on high-resolution MRI slices, with its thickness and articular contact surfaces clearly defined. Subsequently, the geometric models of bones, cartilage, and ligaments were subjected to surface smoothing and topological optimization in Geomagic Studio 2021

(Geomagic Inc., USA) to improve surface quality and ensure numerical stability in subsequent finite element analyses. Anterior cruciate ligament (ACL), posterior cruciate ligament (PCL), medial collateral ligament (MCL), and lateral collateral ligament (LCL) were represented as simplified band-like structures connecting their anatomical attachment sites. These attachment sites were precisely identified based on MRI data to ensure anatomical accuracy. Finally, all processed structures were imported into SolidWorks 2021 (SolidWorks Corp., USA) for assembly and solid modelling (Fig. 1D) [17].

2.5.2 Material properties, boundary and load conditions

The finite element model of the knee joint in this study comprises the distal femur, proximal tibia, proximal fibula, medial and lateral menisci, femoral and tibial cartilage layers, and the four primary knee ligaments (ACL, PCL, MCL, LCL) (Fig. 1E). All structures were meshed in ANSYS Workbench 2024 using four-node linear tetrahedral elements, which provide favorable accuracy and computational efficiency for complex knee joint geometries and contact analyses [23].

To enhance local computational accuracy, bone element sizes were set to approximately 3 mm, cartilage and menisci to approximately 1 mm, and ligaments to 1.5 mm, resulting in a total of 596,829 elements [7]. Local mesh refinement was applied to critical regions such as the femoral–tibial contact interfaces and ligament attachment sites to improve the capture of stress gradients. Mesh independence was validated using a progressive mesh refinement strategy. While maintaining constant mesh partition ratios, the overall mesh size was gradually reduced (approximately 10% per refinement level) to generate models with different mesh densities. The maximum von Mises stress in the femoral and tibial cartilage layers was used as the convergence criterion for comparing computational results across refinement levels. The model was considered converged when the relative difference in key output parameters between two successive mesh levels was less than 5%. The convergence analysis showed that the predicted stresses gradually stabilized with further mesh refinement, indicating that the simulation results were no longer sensitive to mesh size and ensuring the numerical stability and reliability of the model.

Regarding material properties, bone, cartilage, menisci, and ligaments were modelled as linearly elastic, homogeneous, and isotropic materials. This simplification has been widely adopted in knee joint finite element studies and allows reliable biomechanical evaluation while reducing computational cost [24]. The material parameters for each component, including Young’s modulus (E) and Poisson’s ratio (v), are listed in Table 1 [25].

Table 1
Material properties and mesh size of each component.

Component	Young's Modulus E (MPa)	Poisson's Ratio	Mesh size (mm)	Ref.
Bone	12000	0.3	3	[26]
Cartilage	5	0.46	1	[27]
Meniscus	59	0.45	1	[23]
ACL	116	0.3	1.5	[28]
PCL	87	0.3	1.5	[17]
MCL	48	0.3	1.5	[25]
LCL	48	0.3	1.5	[17]

Regarding contact settings, the femoral–tibial cartilage interfaces and cartilage–meniscus interfaces were defined as frictionless surface-to-surface contacts. This approach minimizes numerical errors arising from uncertainty in friction coefficients and allows the analysis to primarily focus on intra-articular load transmission mechanisms. Similarly, frictionless contact was assigned between the menisci and both femoral and tibial cartilage surfaces. Each cartilage layer was fully bonded (tie constraint) to its underlying subchondral bone surface, ensuring numerical stability and reproducibility of the simulations. Regarding boundary conditions, the six degrees of freedom of the distal tibia and fibula were fully constrained [17], serving as the reference for load transmission. To simplify the kinematic constraints of the proximal segment, the superior surface of the femur was coupled to a single reference point, with constraints applied only in the flexion–extension direction. This configuration enabled the model to maintain the physiologically realistic relative alignment between the femur and tibia in the extended position [29]. Prior to simulation, the knee joint was positioned in a neutral alignment to establish the baseline configuration of the model. The joint posture was adjusted by modifying the rotational angle of the femur in the sagittal plane, aligning the femoral mechanical axis with the tibial axis to match the experimentally measured knee joint angle (Fig. 1E) [17]. Subsequently, the static loading conditions corresponding to TIO and TOO landing postures were applied to the two adjusted knee models. Each participant successfully completed seven trials under each landing condition. The kinetic data at the instant of peak knee joint contact force were extracted and averaged for each condition. The resulting mean peak contact force was then applied to the tibial plateau to simulate the intra-articular loading state of the femoral–tibial joint.

2.5.3 Model validation

This study validated the mechanical plausibility and predictive reliability of the knee joint finite element model using multiple approaches. Firstly, the model's anterior–posterior stability was assessed via the classical anterior drawer test [30]. Specifically, with the femur fixed, a 134 N anterior load was applied to

the tibia, resulting in a simulated anterior tibial translation of 4.32 mm. This result is highly consistent with previous finite element studies of the knee under identical or comparable loading conditions. Multiple studies employing three-dimensional finite element models based on anatomical reconstruction have reported that, under a 134 N anterior drawer load, anterior tibial translation in healthy knees typically ranges from approximately 4–6 mm. This range is widely used for the mechanical validation of finite element knee models [31, 32]. For example, Peña et al.'s three-dimensional finite element model of the complete knee. Under the same 134 N load, the model predicted approximately 5.2 mm of anterior tibial translation, which reasonably reflects the ACL's constraining effect on anterior–posterior stability [33]. Compared with these studies, the simulation results of the present study fall within the previously reported reasonable range, indicating that the model demonstrates good credibility in terms of anterior stability and ligament mechanical response.

Furthermore, a high-speed dual fluoroscopic imaging system (DFIS) was used to capture in vivo three-dimensional kinematics of the knee joint during the landing phase. The Coordinate System Calculator plugin in Rhinoceros software (version 6.16, McNeel and Associates, Seattle, WA, USA) was employed to accurately compute knee joint displacement [34]. Subsequently, the projected contours of the finite element model at corresponding flexion angles were spatially registered with the actual X-ray contours. The three-dimensional displacements computed by the model were compared with the kinematic data extracted from DFIS [35]. Results demonstrated high consistency between the model predictions and experimental measurements in both overall motion trends and displacement amplitudes (as shown in Fig. 1F). These findings indicate that the model possesses high fidelity in geometric reconstruction, material parameter assignment, and kinematic driving.

2.6 Statistical analysis

All data were first assessed for normality using the Shapiro–Wilk test. When the assumption of normal distribution was satisfied, a one-way repeated-measures analysis of variance (ANOVA) was performed to examine differences in selected discrete kinematic and kinetic variables of the ankle and knee joints under different toe-pointing conditions [15]. When significant main effects were observed, post hoc pairwise comparisons with Bonferroni correction were conducted. For time-series kinematic and kinetic data, Statistical Parametric Mapping (SPM) paired-sample t-tests were subsequently conducted to evaluate differences across the entire landing phase. The normality assumption for SPM analyses was verified prior to testing, and statistical significance was determined using random field theory (RFT) to account for multiple comparisons across the time series. For cross-correlation analysis, the maximum cross-correlation coefficients (r_{max}) obtained under TIO and TOO conditions were first extracted and then transformed using Fisher's z-transformation to improve normality. The transformed data were subsequently tested for normality, and paired-sample t-tests or Wilcoxon signed-rank tests were applied as appropriate to compare differences in lower limb joint coordination patterns between conditions. The significance level was set at $\alpha = 0.05$. All statistical analyses were performed using MATLAB (R2025b, The MathWorks Inc., Natick, MA, USA) and the SPM1D package.

3 Results

3.1 Knee and ankle joint kinematics, kinetics, and COM characteristics

Figure 2 illustrates the differences in biomechanical characteristics of the knee and ankle joints, as well as the COM, during the landing phase of the badminton lunge under two distinct toe orientation conditions. Results show that compared with TOO landing, TIO landing significantly increased ankle dorsiflexion and eversion angles throughout the stance phase ($p < 0.001$).

For knee joint angles, the abduction angle during the initial 0–5% and terminal 80–100% phases were significantly greater for TOO landing than for TIO landing ($p = 0.048$ and $p = 0.007$, respectively). Regarding vertical joint reaction forces, both ankle and knee reaction forces were significantly greater under TIO landing conditions. Specifically, ankle joint reaction forces showed significant differences only during the late phase (94–100%) ($p = 0.045$), while knee joint reaction forces also exhibited significant differences during the same phase (94–100%) ($p = 0.045$). For anterior–posterior shear forces, ankle shear force during the initial 0–5% phase was significantly greater in TOO landing than in TIO landing ($p = 0.045$). Knee shear forces during the mid-phase (8–83%) and terminal phase (94–100%) were also significantly greater in TOO landing compared with TIO landing ($p < 0.05$ across the stance phase).

For GRF, TOO landing produced significantly greater GRF than TIO landing during the initial 0–5% phase ($p = 0.048$), whereas during the terminal 90–100% phase, GRF was significantly lower for TOO landing than for TIO landing ($p = 0.038$). Additionally, significant differences were observed in COM displacement between the two landing conditions. During TIO landing, sagittal plane displacement was significantly greater than during TOO landing ($p = 0.023$), whereas in the coronal plane, TOO landing resulted in significantly greater COM displacement than TIO landing ($p = 0.042$).

3.2 Cross-correlation analysis results

As shown in Fig. 3, significant differences in maximum cross-correlation coefficients between the two toe orientations were observed for the following variable pairs: COMx-KEX ($p = 0.041$), COMx-KSF ($p = 0.042$), ADF-ARF ($p = 0.003$), ADF-KSF ($p = 0.038$), AEV-KEX ($p = 0.001$), AEV-KAB ($p = 0.003$), and AEV-ASF ($p = 0.026$) ($p < 0.05$). Specifically, for COMx-KEX, the maximum cross-correlation coefficient was 0.992 for TOO and 0.977 for TIO. For COMx-KSF, the values were 0.521 (TOO) and 0.811 (TIO). For ADF-ARF, coefficients were 0.291 (TOO) and − 0.468 (TIO); for ADF-KSF, -0.520 (TOO) and − 0.814 (TIO). For AEV-KEX, coefficients were 0.996 (TOO) and 0.971 (TIO); for AEV-KAB, -0.988 (TOO) and − 0.946 (TIO); and for AEV-ASF, -0.949 (TOO) and − 0.840 (TIO). Additionally, KEX-KSF showed 0.559 (TOO) and 0.808 (TIO).

Overall, the maximum cross-correlation coefficients ranged widely across both TIO and TOO postures, encompassing both strong positive and strong negative correlations. This indicates that the temporal

correlation strength between different variable pairs varies considerably. Statistically significant differences were observed in a relatively limited number of variable pairs, primarily those involving joint angles and joint forces.

3.3 FEA results for the knee joint

As shown in Fig. 4, the finite element analysis demonstrated distinct stress distribution patterns between the TIO and TOO conditions. Regarding the cruciate ligaments, both the ACL and PCL showed pronounced stress concentration in both TIO and TOO, predominantly in the mid-portion and attachment regions. Compared to TOO, overall stress levels and peak stresses of the ACL and PCL were higher under TIO, with high-stress zones more extensively distributed. Conversely, under TOO, stress levels decreased, and stress was more localized with lower peak values. Among the collateral ligaments, both the MCL and LCL displayed localized high-stress regions under both conditions. Under TIO, maximum stresses and high-stress areas were more pronounced, whereas under TOO, stress levels were lower and high-stress regions were smaller. FEA of the menisci revealed that both the MM and LM experienced substantial stress during the landing phase. Under TIO, overall stresses were higher, with high-stress zones concentrated in the main body of the menisci. In contrast, under TOO, stress distribution was more uniform with lower peak stress. For tibial cartilage, both MTC and LTC exhibited annular or locally concentrated stress patterns in both TIO and TOO conditions. Maximum stresses and high-stress coverage were higher under TIO, whereas overall stress levels and high-stress regions were reduced under TOO.

4 Discussion

4.1 Biomechanical characteristics of the knee and ankle joints and COM displacement

The present study demonstrates that toe orientation substantially influences lower-limb biomechanical responses during badminton lunge landings, not merely by altering loading magnitude, but by reorganizing load transmission pathways and movement control strategies across the kinetic chain.

Under TIO conditions, landing was characterized by significantly greater ankle dorsiflexion and eversion, as well as increased joint reaction forces, particularly during the late landing phase. This indicates that impact attenuation under TIO is initiated predominantly at the ankle joint, while the knee assumes a secondary role in regulating residual loads and maintaining postural stability. This is consistent with previous findings suggesting that increased ankle dorsiflexion and eversion may compromise joint stability and elevate ligament loading demands [15]. The concurrent increase in knee joint reaction forces and sagittal-plane COM displacement further indicates that greater forward momentum and loading are sustained during late landing.

By contrast, TOO landings exhibited lower overall joint reaction forces but greater knee abduction angles and higher anterior–posterior shear forces at the knee during the landing phase. This indicates that mechanical demand is redistributed through changes in joint alignment and force direction, rather than being uniformly reduced. Previous studies have shown that increased knee abduction during landing is associated with elevated ACL loading [36]. However, the present findings do not fully support this relationship, as increased knee abduction under TOO was accompanied by reduced overall loading and tissue stress, suggesting a compensatory load redistribution mechanism rather than a direct increase in injury-related loading. Additionally, the greater coronal-plane COM displacement observed under TOO indicates increased demands on lateral stability control.

Although TOO reduces overall joint reaction forces and internal stress levels, the increased anterior–posterior shear forces at the knee suggest that mechanical demand is redistributed rather than uniformly reduced, which may have implications for specific structures such as the ACL. Taken together, these findings point to two distinct impact attenuation strategies: TIO favors a more localized, ankle-driven absorption pattern, whereas TOO promotes a redistribution of loads through multi-planar control and joint alignment adjustments. Importantly, although TIO was associated with higher joint reaction forces, the present cross-sectional design does not allow inference of long-term injury risk, and these findings should be interpreted as differences in acute mechanical demand rather than direct indicators of injury.

4.2 Cross-correlation analysis

Cross-correlation analysis revealed that toe orientation significantly affects coordination patterns within the lower-limb kinetic chain, particularly in the coupling between COM motion, ankle kinematics, and knee joint loading.

Among COM-related variables, COMx exhibited stronger correlations with knee flexion–extension angles and shear forces under TIO, indicating tighter temporal synchronization and a more direct involvement of the knee in postural control. This suggests a more active role of the knee within the lower-limb kinetic chain, rather than a purely passive transmission of forces [36, 37]. In contrast, under TOO conditions, ankle–knee coordination was more pronounced, suggesting a distributed, multi-joint load-sharing strategy that facilitates impact attenuation [38]. Directional changes in correlation magnitude and sign (e.g., ADF–ARF shifting from positive to negative) further indicate that toe orientation alters not only the strength but also the structure of inter-joint coordination, reflecting fundamentally different movement control strategies [11].

Mechanistically, TIO landings appear to rely more on ankle-dominant impact absorption followed by localized knee-mediated load regulation, whereas TOO promotes coordinated multi-joint responses that distribute mechanical loads more evenly.

4.3 FEA of the knee joint

At the tissue level, the finite element results provide further insight into these biomechanical differences. Compared with TOO, TIO consistently resulted in higher von Mises stress levels across all evaluated knee joint tissues, including the ACL, PCL, collateral ligaments, menisci, and tibial cartilage, with more extensive high-stress regions. Previous finite element studies on jump and change-of-direction landings indicate that cruciate ligaments are among the first structures to experience high stress when the knee assumes greater postural stabilization responsibilities [39]. Importantly, these increases were not limited to a single structure but occurred concurrently across multiple tissues, indicating a multi-tissue loading pattern within the knee joint. Medial structures such as the MCL and medial meniscus are particularly sensitive to changes in lower-limb alignment and rotational loads, explaining their vulnerability under TIO [40]. This suggests that under TIO conditions, mechanical demand is less effectively redistributed, leading to a more concentrated internal stress environment. In contrast, TOO was associated with lower peak stresses and more localized stress distributions across all structures. This more uniform stress pattern is consistent with the enhanced inter-joint coordination observed in the cross-correlation analysis, suggesting that improved coordination may facilitate more effective load dispersion.

However, it is important to emphasize that the present study does not establish physiological or injury thresholds for these stress values. Therefore, it remains unclear whether the observed stress levels fall within normal physiological ranges or approach levels associated with tissue damage. As such, these findings should be interpreted as relative differences in mechanical loading rather than direct evidence of increased injury risk. Overall, the combined evidence from kinematic, coordination, and finite element analyses suggests that TIO promotes a more localized and concentrated loading pattern, whereas TOO supports a more distributed load-sharing mechanism within the knee joint.

4.4 Research limitations and future prospects

Despite these findings, several limitations should be considered when interpreting the results. First, the sample did not consider gender or athletic level differences, which may affect joint loading and coordination. Second, the cross-sectional design focused on a single landing event, limiting inference on cumulative loading and long-term injury risk. The experimentally controlled toe orientations may represent relatively extreme postures, and their frequency in real match scenarios remains unclear. Additionally, cross-correlation analysis reflects temporal associations rather than direct neuromuscular control, and finite element analysis estimates tissue stress without capturing in vivo injury thresholds. Future studies should incorporate in-game motion capture and wearable sensors to enhance ecological validity, and integrate subject-specific thresholds or fatigue-related loading for more physiologically meaningful interpretations of mechanical risk.

5 Conclusion

Research findings indicate that different toe orientations significantly alter lower-limb biomechanical responses during the landing phase of a badminton lunge. These effects extend beyond individual joints, reflecting changes in load transmission and coordination patterns across the lower-limb kinetic chain. TIO posture tends to promote a more localized, load-bearing–dominant strategy, with greater

mechanical demand on the knee joint and increased concurrent loading across ligaments, menisci, and cartilage. Conversely, TOO posture facilitates a more distributed load-sharing strategy through joint alignment and inter-joint coordination, resulting in reduced stress concentration within knee tissues. These findings suggest that foot landing posture may influence knee joint loading through its effect on kinetic chain coordination, rather than acting as an isolated local factor. This provides a biomechanical basis for optimizing landing techniques in badminton and may inform training and rehabilitation strategies aimed at reducing lower-limb loading demands.

Abbreviations

ACL
Anterior cruciate ligament
ADF
Ankle dorsiflexion angle
AEV
Ankle eversion angle
ARF
Ankle reaction force
ASF
Ankle sagittal-plane shear force
COM
Center of mass
COMx
Anterior–posterior displacement of the center of mass
COMy
Medial–lateral displacement of the center of mass
DFIS
Dual fluoroscopic imaging system
FEA
Finite element analysis
GRF
Ground reaction force
KAB
Knee abduction angle
KEX
Knee extension angle
KRF
Knee reaction force
KSF
Knee sagittal-plane shear force

LCL
Lateral collateral ligament
LM
Lateral meniscus
LTC
Lateral tibial cartilage
MCL
Medial collateral ligament
MM
Medial meniscus
MTC
Medial tibial cartilage
PCL
Posterior cruciate ligament
SPM
Statistical Parametric Mapping
TIO
Toe-in orientation
TOO
Toe-out orientation

Declarations

Ethics approval and consent to participate

The present study received ethical approval from the Ethical Committee of Ningbo University (Approval No. TY 2025051). All procedures involving human participants were conducted in accordance with the Declaration of Helsinki, as well as the applicable local legislation and institutional requirements. Written informed consent was obtained from all participants prior to their participation in the study.

Consent for publication

Not applicable.

Competing interests

The authors declare no competing interests.

Author Contribution

Jun Wen: Conceptualization, Methodology, Formal analysis, Writing – original draft. Zilong Lu: Investigation, Data curation, Writing – review & editing. Zirui Yin: Methodology, Software, Formal analysis,

Writing – review & editing. Pengbin Tong: Methodology, Software, Formal analysis, Writing – review & editing. Enze Shao: Validation, Visualization, Writing – review & editing. Bálint Kovács: Investigation, Data curation, Writing – review & editing. Dong Sun: Resources, Software, Writing – review & editing. Yang Song: Resources, Software, Writing – review & editing. Tibor J. Goda: Formal analysis, Visualization, Writing – review & editing. Fei Zheng: Supervision, Project administration, Writing – review & editing. Junxia Lin: Supervision, Methodology review, Writing – review & editing. Peng Yang: Conceptualization, Funding acquisition, Supervision, Formal analysis, Writing – review & editing.

Funding

This study was sponsored by National Key R&D Program of China (2024YFC3607305), Joint Fund of Zhejiang Provincial Natural Science Foundation of China (LKLY26H170001), Zhejiang Provincial Key Project of Education Science Planning (2025SB084), Scientific Research Fund of Zhejiang Provincial Education Department (Y202559510), Ningbo Key Research and Development Program (2022Z196), Zhejiang Rehabilitation Medical Association Scientific Research Special Fund (ZKKY2023001), Research Academy of Medicine Combining Sports, Ningbo (No.2023001), Ningbo Clinical Research Center for Orthopedics and Exercise Rehabilitation (No.2024L004), and K. C. Wong Magna Fund in Ningbo University.

Data Availability

The datasets generated and analyzed during the current study are not publicly available due to the ongoing nature of the associated research projects, but are available from the corresponding author on reasonable request.

References

1. Phomsoupha M, Laffaye G. The science of badminton: game characteristics, anthropometry, physiology, visual fitness and biomechanics. Sports Med. 2015;45(4):473–95. 10.1007/s40279-014-0287-2.
2. Phomsoupha M, Laffaye G. Injuries in badminton: A review. Sci Sports. 2020;35(4):189–99. 10.1016/j.scispo.2020.01.002.
3. Xie Z, Wu X, Liang H, Li W, Li R, Wang Z, et al. Effects of eight-week resistance and complex training on the biomechanical characteristics of lower limbs during badminton backhand forward lunge. Front Sports Act Living. 2025;7:1615558. 10.3389/fspor.2025.1615558.
4. Lam W-K, Wong DW-C, Lee WC-C. Biomechanics of lower limb in badminton lunge: a systematic scoping review. PeerJ. 2020;8:e10300. 10.7717/peerj.10300.
5. Zhu X, Wei F, Li S, Zhang T, Shen P, Fong DT, et al. Toe-out landing reduces anterior talofibular ligament strain while maintains calcaneofibular ligament strain in people with chronic ankle

instability. J Sport Health Sci. 2025;14:101035. 10.1016/j.jshs.2025.101035.

6. Teng PSP, Kong PW, Leong KF. Effects of foot rotation positions on knee valgus during single-leg drop landing: Implications for ACL injury risk reduction. Knee. 2017;24(3):547–54. 10.1016/j.knee.2017.01.014.
7. Qu X, Xu D, Yang X, Ugbolue UC, Zhou H, Gu Y. Exploring the Relationship Between Foot Position and Reduced Risk of Knee-Related Injuries in Side-Cutting Movements. Appl Sci. 2024;14(23):11295. 10.3390/app142311295.
8. Dubois O, Roby-Brami A, Parry R, Khoramshahi M, Jarrassé N. A guide to inter-joint coordination characterization for discrete movements: a comparative study. J Neuroeng Rehabil. 2023;20(1):132. 10.1186/s12984-023-01252-2.
9. Lilley T, Herb CC, Hart J, Hertel J. Lower extremity joint coupling variability during gait in young adults with and without chronic ankle instability. Sports Biomech. 2018;17(2):261–72. 10.1080/14763141.2017.1287215.
10. Williams LR, Arch ES, Bruening DA. Kinetic coupling in distal foot joints during walking. J Foot Ankle Res. 2023;16(1):44. 10.1186/s13047-023-00643-x.
11. Dadfar M, Sheikhhoseini R, Jafarian M, Esmaeili A. Lower extremity kinematic coupling during single and double leg landing and gait in female junior athletes with dynamic knee valgus. BMC Sports Sci Med Rehabil. 2021;13(1):152. 10.1186/s13102-021-00385-y.
12. Hiratsuka S, Takabayashi T, Watanabe T, Kikumoto T, Kubo M. Classification of Kinematic Coupling Patterns Between Lower Limb Joints During Running. J Orthop Res. 2025;43(6):1171–8. 10.1002/jor.26074.
13. Kawabata R, Yokoyama M, Matsumoto Y, Kubota K, Kosuge S, Sunaga Y, et al. Lower limb biomechanics and control of center of mass during turning phases in daily gait. J Electromyogr Kinesiol. 2025;80:102959. 10.1016/j.jelekin.2024.102959.
14. Wang TM, Chen HL, Hsu WC, Liu MW, Lu TW. Biomechanical Role of the Locomotor System in Controlling Body Center of Mass Motion in Older Adults During Obstructed Gait. Med (Mex). 2011;26(2):195–203. 10.1017/s1727719100003051.
15. Wen J, Xu D, Gao X, Qu X, Zhang Z, Zhou H, et al. Effects of foot rotation on ankle control and injury risk during badminton lunge landings. BMC Sports Sci Med Rehabil. 2025;17(1):341. 10.1186/s13102-025-01393-y.
16. DeJong AF, Koldenhoven RM, Hertel J. Hip biomechanical alterations during walking in chronic ankle instability patients: a cross-correlation analysis. Sports Biomech. 2022;21(4):460–71. 10.1080/14763141.2021.1884285.
17. Li F, Sun D, Song Y, Zhou Z, Wang D, Cen X, et al. Dynamic simulation of knee joint mechanics: individualized multi-moment finite element modelling of patellar tendon stress during landing. J Biomech. 2025;186:112730. 10.1016/j.jbiomech.2025.112730.
18. Mei Q, Gu Y, Fu F, Fernandez J. A biomechanical investigation of right-forward lunging step among badminton players. J Sports Sci. 2017;35(5):457–62. 10.1080/02640414.2016.1172723.

19. Wen J, Xu D, Zhou H, Zhang Z, Xiang L, Munivrana G, et al. Analysis of Quadriceps Fatigue Effects on Lower Extremity Injury Risks During Landing Phases in Badminton Scissor Jump. Sensors. 2025;25(8):2536. 10.3390/s25082536.
20. Sinclair J, Taylor PJ, Hobbs SJ. Digital filtering of three-dimensional lower extremity kinematics: An assessment. J Hum Kinetics. 2013;39:25. 10.2478/hukin-2013-0065.
21. Winter DA. Biomechanics and motor control of human movement. Wiley; 2009.
22. Shao E, Mei Q, Ye J, Ugbolue UC, Chen C, Gu Y. Predicting coordination variability of selected lower extremity couplings during a cutting movement: An investigation of deep neural networks with the LSTM structure. Bioengineering. 2022;9(9):411.
23. Kiapour A, Kiapour AM, Kaul V, Quatman CE, Wordeman SC, Hewett TE, et al. Finite element model of the knee for investigation of injury mechanisms: development and validation. J Biomech Eng. 2014;136(1). 10.1115/1.4025692.
24. Yan M, Liang T, Zhao H, Bi Y, Wang T, Yu T, et al. Model properties and clinical application in the finite element analysis of knee joint: a review. Orthop Surg. 2024;16(2):289–302. 10.1111/os.13980.
25. Galbusera F, Freutel M, Dürselen L, D'Aiuto M, Croce D, Villa T, et al. Material models and properties in the finite element analysis of knee ligaments: a literature review. Front Bioeng Biotechnol. 2014;2:54. 10.3389/fbioe.2014.00054.
26. Balaji V, Rajesh D, Murugu Nachippan N, Maridurai T, Sathish T, Balakrishnan E. Finite element analysis of a human foot. Sports Med. 2021;46:4265–70. 10.1016/j.matpr.2021.03.069.
27. Wang Y, Li Z, Wong DW-C, Cheng C-K, Zhang M. Finite element analysis of biomechanical effects of total ankle arthroplasty on the foot. J Orthop Transl. 2018;12:55–65. 10.1016/j.jot.2017.12.003.
28. Park S, Lee S, Yoon J, Chae SW. Finite element analysis of knee and ankle joint during gait based on motion analysis. Med Eng Phys. 2019;63:33–41. 10.1016/j.medengphy.2018.11.003.
29. Gao Z, Xiang L, Jiang H, Mei Q, Fekete G, Baker JS, et al. Musculoskeletal modelling sequentially integrated with stress simulation reveals asymmetrical knee loading and ligament stress during long-distance running. BMC Sports Sci Med Rehabil. 2025;17(1):337. 10.1186/s13102-025-01372-3.
30. Makhmalbaf H, Moradi A, Ganji S, Omidi-Kashani F. Accuracy of lachman and anterior drawer tests for anterior cruciate ligament injuries. Archives Bone Joint Surg. 2013;1(2):94.
31. Butler DL, Noyes FR, Grood ES. Ligamentous restraints to anterior-posterior drawer in the human knee. A biomechanical study. J Bone Joint Surg Am Volume. 1980;62(2):259–70.
32. Li G, Suggs J, Gill T. The effect of anterior cruciate ligament injury on knee joint function under a simulated muscle load: a three-dimensional computational simulation. Ann Biomed Eng. 2002;30(5):713–20. 10.1114/1.1484219.
33. Pena E, Calvo B, Martinez M, Doblare MJJ. A three-dimensional finite element analysis of the combined behavior of ligaments and menisci in the healthy human knee joint. J Biomech. 2006;39(9):1686–701. 10.1016/j.jbiomech.2005.04.030.

34. Shu J, Zheng N, Teng H, Tsai TY, Liu Z. In vivo biomechanical dynamic simulation of a healthy knee during the single-leg lunge and its experiment validation. Med Eng Phys. 2024;129:104183. 10.1016/j.medengphy.2024.104183.
35. Zhu Z, Li G. An automatic 2D-3D image matching method for reproducing spatial knee joint positions using single or dual fluoroscopic images. Comput Methods Biomech Biomed Engin. 2012;15(11):1245–56. 10.1080/10255842.2011.597387.
36. Yeap MW, Ramasamy Y, Usman J, King M, Razman R. Knee Abduction Angles and Landing Kinematics in Badminton Jump Smash: A Study of ACL Injury Risk Factors. Bioengineering. 2025;12(4):343. 10.3390/bioengineering12040343.
37. Belkhelladi M, Cierson T, Martineau PA. Biomechanical Risk Factors for Increased Anterior Cruciate Ligament Loading and Injury: A Systematic Review. Orthop J Sports Med. 2025;13(2):23259671241312681. 10.1177/23259671241312681.
38. Sarvestan J, Fakhraei Rad N. Lower Limb Joint Coordination and Coordination Variability During Landing: A Scoping Review. Appl Sci. 2025;15(9). 10.3390/app15095118.
39. Shi H, Yu Y, Huang H, Li H, Ren S, Ao YJB. Biomechanical Determinants of Anterior Cruciate Ligament Stress in Individuals Post–ACL Reconstruction During Side-Cutting Movements. Bioengineering. 2025;12(3):222. 10.3390/bioengineering12030222.
40. Ghiretti R, Panzavolta F, Lucidi GA, Zaffagnini S. Combined ACL–MCL Injuries: Anatomy, Biomechanics, and Clinical Management. J Mech. 2025;61(10):1788. 10.3390/medicina61101788.

Figures

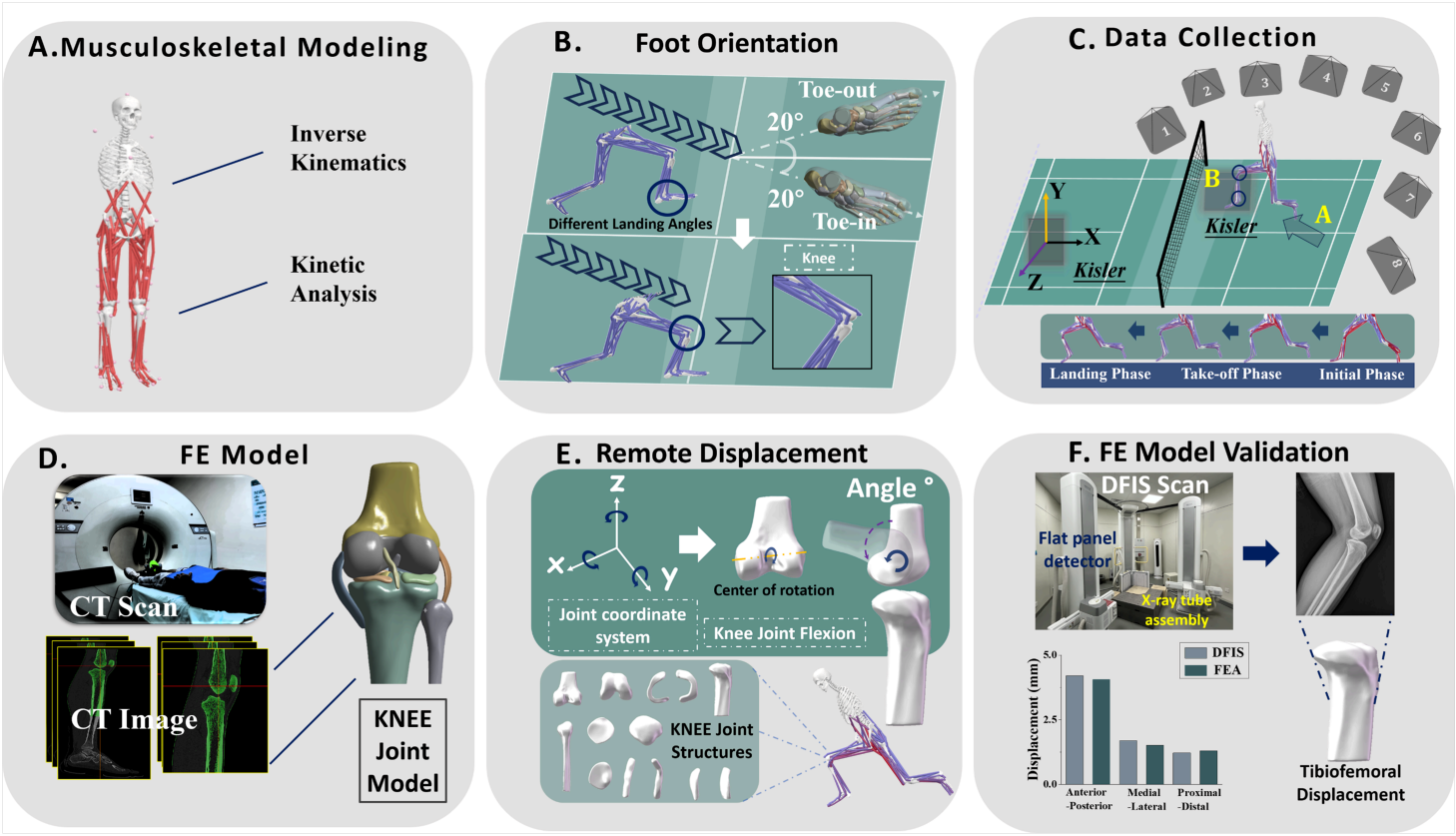


Figure 1

Overview of the experimental protocol, finite element model construction, and validation. (A) Schematic illustration of anatomical marker placement. (B) Representative knee and ankle joint configurations during landing under different ankle orientations. (C) Testing workflow and the badminton right-lunge movement protocol. (D) CT imaging and knee joint modeling procedure. (E) Components of the knee joint finite element model and the loading and boundary conditions applied in ANSYS Workbench. (F) Validation illustrations: dual-plane fluoroscopy–based verification of the finite element model; results showing the comparison between predicted and measured joint kinematics.

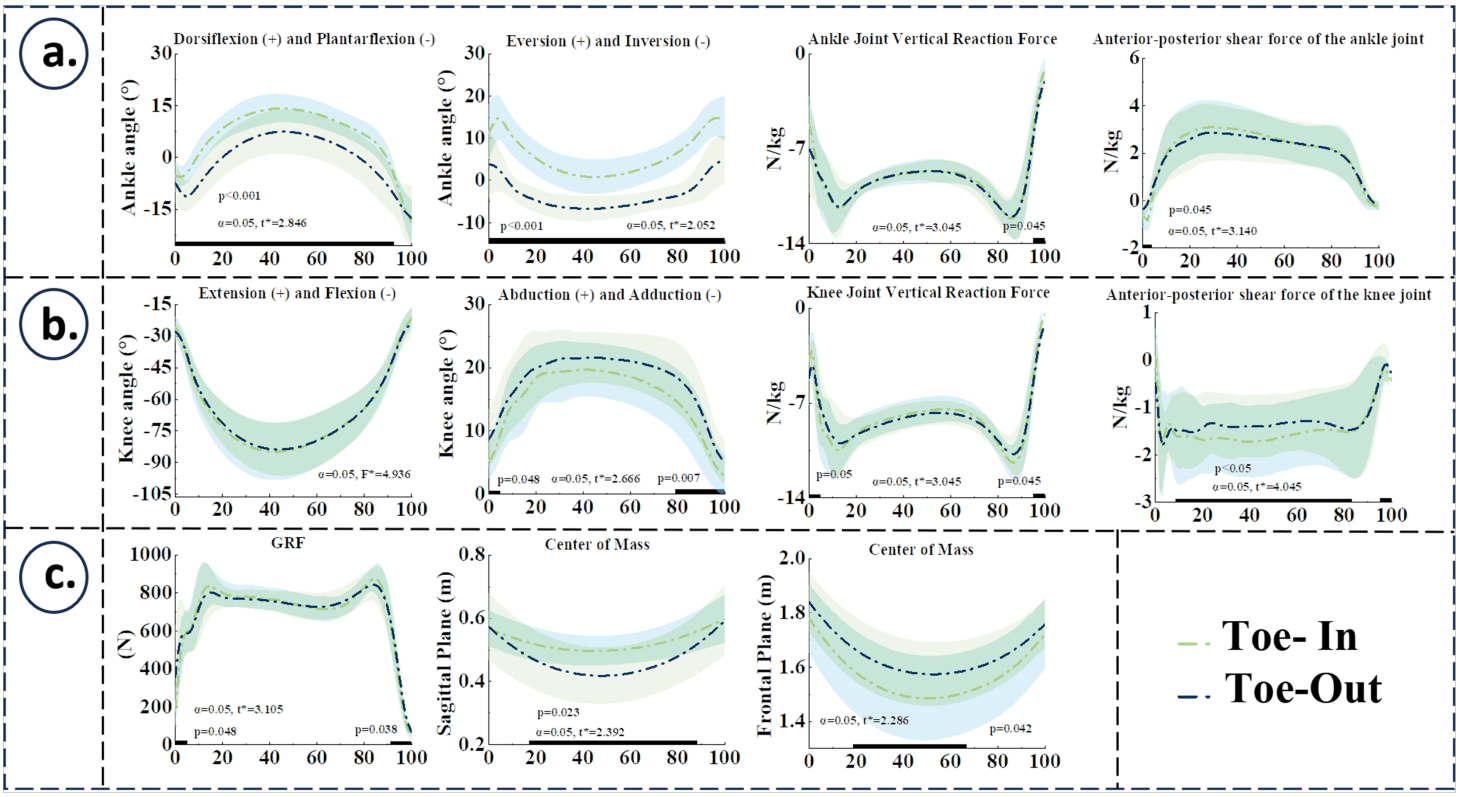


Figure 2

Changes in lower limb biomechanical characteristics during the landing phase of a badminton lunge under different toe orientations. (A) Kinematic and kinetic results of the ankle joint. (B) Kinematic and kinetic results of the knee joint. (C) COM and GRF. SPM analysis highlights characteristic differences in ankle and knee joints, COM displacement, and GRF. Green and blue lines indicate toe-in and toe-out conditions during lunge landing, respectively.

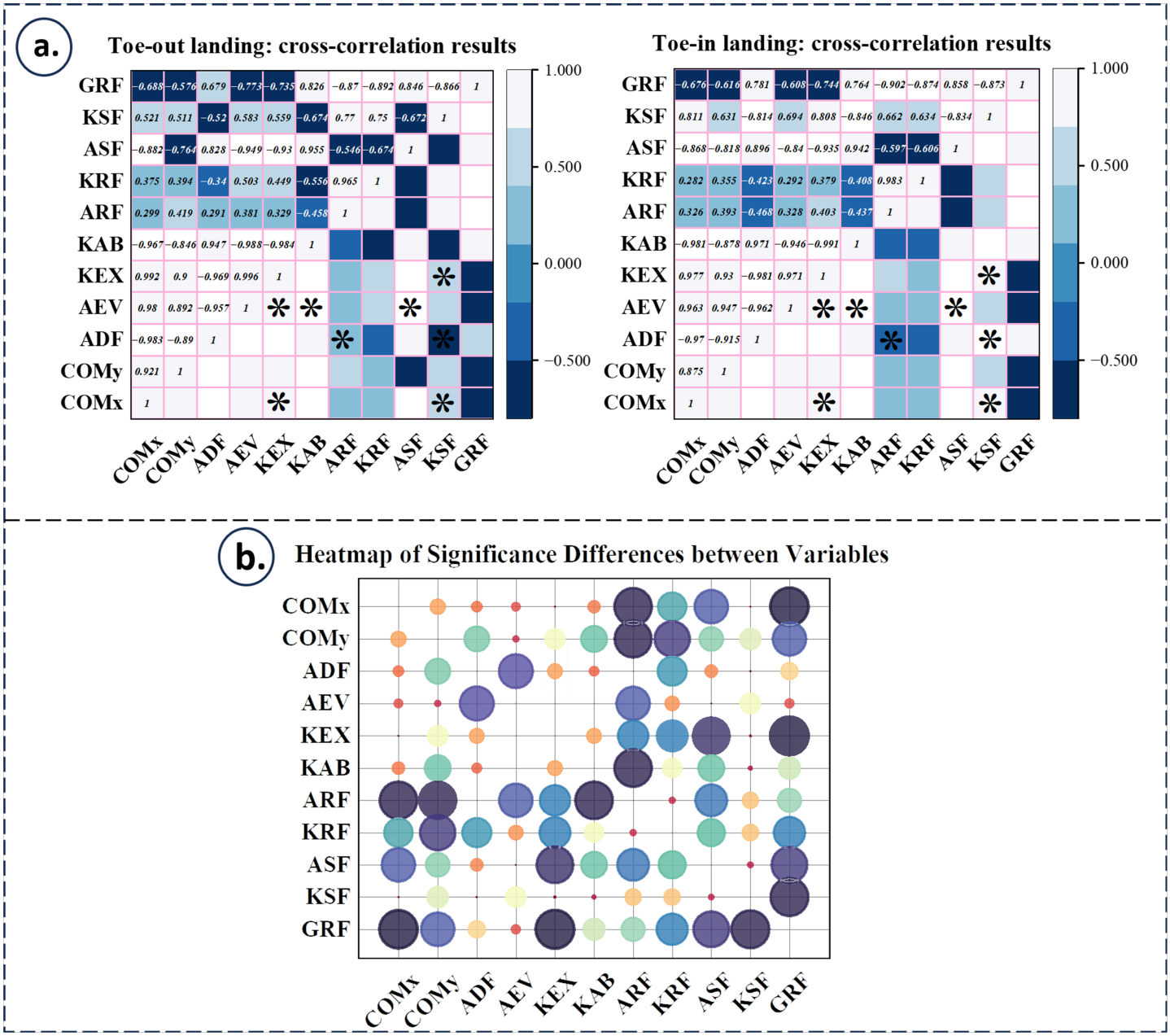


Figure 3

Schematic representation of the cross-correlation analysis results. Figures 3A and 3B show the maximum cross-correlation coefficient matrices under toe-out and toe-in conditions, respectively, where '*' indicates variable pairs exhibiting significant differences in maximum cross-correlation coefficients between the two toe orientations. Figure 3C shows the p-value distributions for the differences in maximum cross-correlation coefficients across all variable pairs.

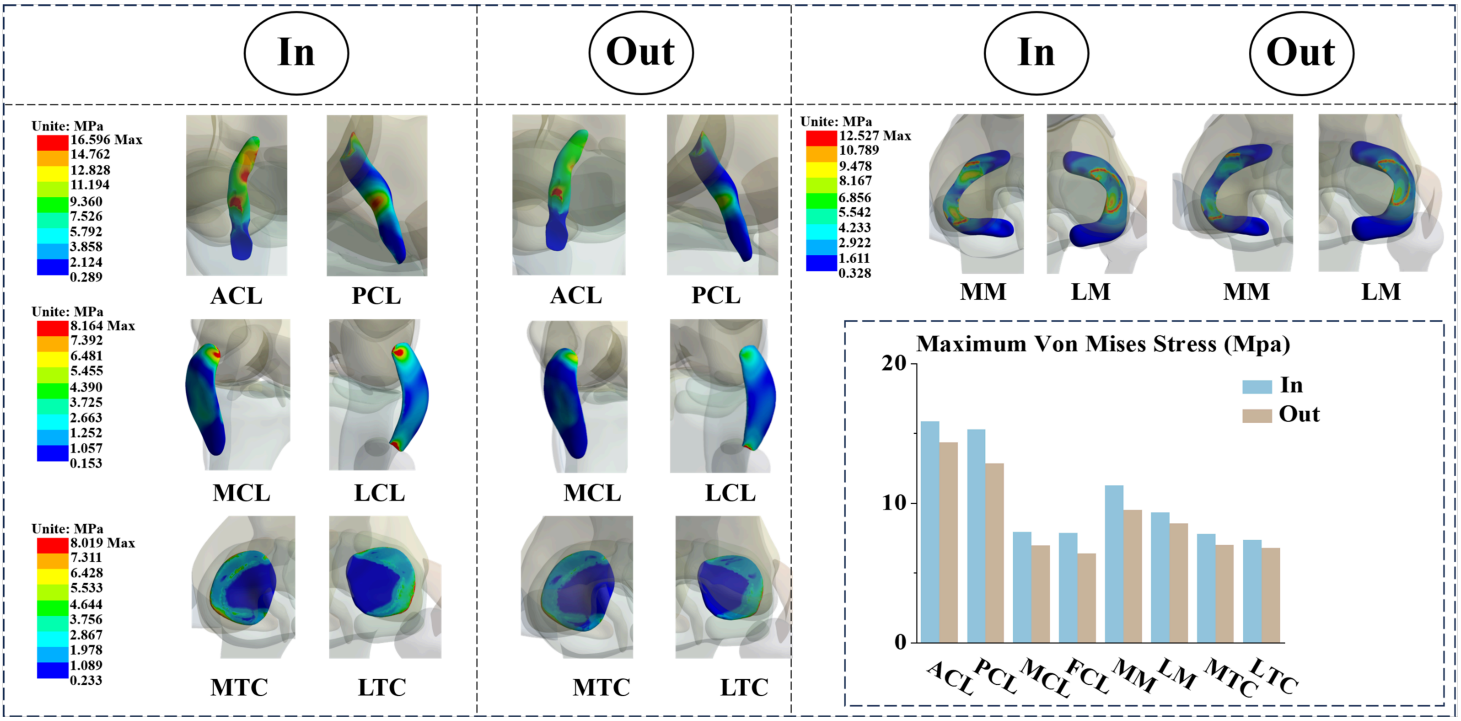


Figure 4

Finite Element Analysis results and peak stress comparisons for the knee joint during the landing phase of a badminton lunge under different toe orientation conditions. The left panel shows von Mises stress distributions across key knee structures—including the ACL, PCL, MCL, LCL, MM, LM, MTC, and LTC. Colors range from blue to red, representing stress levels from low to high. The right panel presents a bar chart comparing peak von Mises stresses across all tissue structures under different toe orientations, quantifying the effect of landing posture on internal knee joint biomechanical loading.